Using muons to probe the vortex lattice in superconductors

Steve Lee

University of St Andrews, Scotland

1 Introduction

Muon spin rotation (μSR) is a particularly useful technique with which to study superconductors, particularly the mixed state. As a microscopic probe it can obtain structural information not accessible to macroscopic methods such as magnetisation measurements. It should nonetheless also be viewed as a probe of the bulk properties, since the muon typically penetrates 100–200μm into the sample. Perhaps most importantly it is normally used to sample the *equilibrium* properties of the vortex state, and in general is a non-disruptive probe, although there are some exceptions. μSR also carries some advantages over NMR in that in principle any applied field may be used, which is important for investigating field dependent properties, especially in exotic vortex systems. While to date the use of muons to study superconductors has been almost exclusively confined to the mixed state, recent advances in the production of ultra low momentum muons could make possible the investigation of superconductivity at surfaces and interfaces in the Meissner state. This chapter will, however, be concerned with the more usual investigation of the mixed state.

2 The mixed state of superconductors

In a type II superconductor there exist two distinct magnetic phases. Below the lower critical field H_{c_1} resistanceless currents flow in a thin region at the surface of a superconductor to create a magnetisation $\mathbf{M}$ of the sample equal and opposite to the applied magnetic field, $\mathbf{H}_a = -\mathbf{M}$. There is thus a net zero flux density inside the bulk of the material, that is $\mathbf{B} = \mu_0(\mathbf{H}_a + \mathbf{M}) = 0$. Above H_{c_1} but below the upper critical field H_{c_2}, at which the material becomes a normal metallic conductor, there exists a phase region known as the mixed state. In this phase flux is allowed to penetrate the bulk of the material, but only in the form of microscopic supercurrent vortices known as flux lines, which extend throughout the sample. Each vortex line carries one quantum of flux

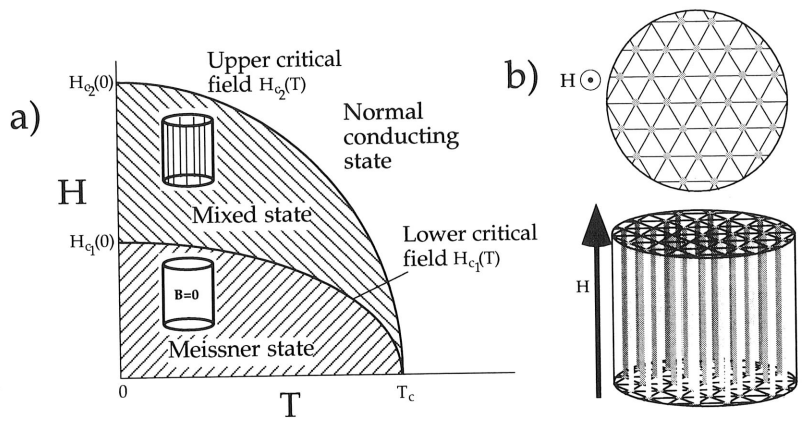

Figure 1. *(a) The magnetic phase diagram of a type II superconductor. (b) In the mixed state flux lines can penetrate the bulk of the sample and form a flux-line lattice.*

$\Phi_0 = h/2e$ (where h is Planck's constant and e is the charge of an electron). Due to electromagnetic interactions between flux lines, these flux vortices arrange themselves on a two dimensional periodic lattice (Figure 1), which is usually of hexagonal symmetry (Tinkham 1975). Square lattices are also found, and in exotic superconductors there exists a range of other possible vortex arrangements, some of which we will discuss later.

It is convenient at this stage to introduce some characteristic length scales associated with the superconducting state and the vortex lattice. The superconducting state may be described by a macroscopic wavefunction $\Psi(r)$, which may undergo spatial variations on the scale of the superconducting coherence length ξ (Figure 2). An isolated vortex consists of a core of normal electrons outside of which flow the supercurrents which constitute the flux line. Since $\Psi(r)$ must thus go to zero at the centre of the vortex, ξ effectively defines the radius of the vortex core. The supercurrents are able to screen a static applied magnetic field over a length scale of the superconducting penetration depth $\lambda(T)$. This is analogous to the screening length of a normal conductor in an AC magnetic field. The magnetic extent of a vortex line is thus characterised by the penetration depth λ, which may be related to the density n_s and effective mass m^* of the superconducting charge carriers via $n_s/m^* \propto \lambda^{-2}$ (Tinkham 1975). In the London limit the coherence length ξ

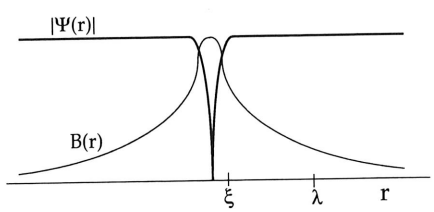

Figure 2. *Schematic representation of a vortex line, showing the characteristic length scales ξ and λ, and the spatial variation of the order parameter $\Psi(r)$ and the internal flux density $B(r)$. The core size is effectively defined by ξ.*

is taken as being vanishingly small, and the variation of the magnetic field around an isolated vortex line is given by:

$$B(r) = \frac{\Phi_0}{2\pi\lambda^2} K_0\left(\frac{r}{\lambda}\right) \tag{1}$$

where K_0 is a Hankel function of zero order (Tinkham 1975). This function can be approximated over certain ranges of r as:

$$B(r) \rightarrow \frac{\Phi_0}{2\pi\lambda^2} \ln\left(\frac{\lambda}{r}\right) \qquad \text{for } \xi \ll r \ll \lambda$$

$$B(r) \rightarrow \frac{\Phi_0}{2\pi\lambda^2}\sqrt{\frac{\lambda}{r}} \exp\left(-\frac{r}{\lambda}\right) \qquad \text{for } r \gg \lambda$$

For fields somewhat above H_{c_1} the typical separation between flux lines $a < \lambda$, so the flux lines strongly overlap. Since each flux line carries Φ_0 of flux, the average internal flux density is given by $B = \sqrt{3}\Phi_0/2a^2$ for a triangular lattice, or simply $B = \Phi_0/a^2$ for a square one.

The μSR technique is, under some circumstances, able to say something about all of the above characteristic length scales λ, ξ and a. It should at this stage be stressed, however, that these quantities are determined by making measurements on the vortex lattice in the mixed state. It is therefore crucial that the one understands the nature of the vortex state in a given material before interpreting μSR signals to extract values for these parameters. In the following section we will discuss how these parameters may be determined in the simplest case where an ideal vortex lattice is assumed.

3 The μSR signal from an ideal vortex line lattice

Studies of the vortex lattice are almost exclusively performed with the incoming muon polarisation transverse to the applied field, as illustrated in Figure 3(a). Since the magnetic length scales are in general much larger than the atomic spacing, the incoming muons randomly sample the internal flux density. The spatial variations of $B(r)$ thus give rise to

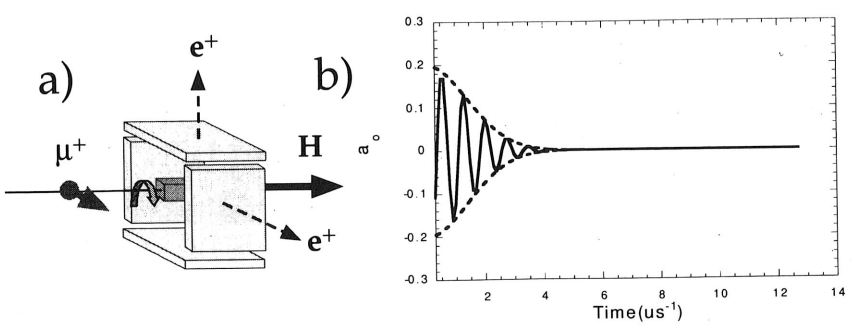

Figure 3. *Schematic representation of (a) the geometry of the transverse μSR experiment and (b) the damped signal arising from the presence of a vortex line lattice, after removing the effects of the muon lifetime.*

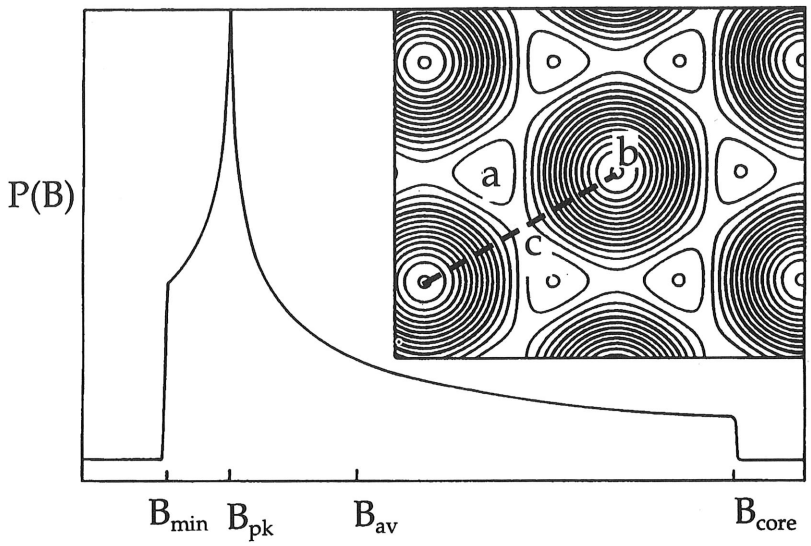

Figure 4. *The probability distribution $p(B)$ of the internal flux density of the vortex line lattice. The details will vary according to the symmetry of the lattice (triangular or square) and the values of ξ, λ and a. The general form will however always be broadly similar, and the features shown can be regarded as generic (see text).*

a damping of the muon spin precession signal, as illustrated schematically in Figure 3(b). The form of this damping intimately reflects the details of vortex lattice. The Fourier transform of the time decay signal gives the probability density $p(B)$ of the internal flux density, an example of which is given in Figure 4. Several distinctive features may be identified in such a lineshape. Firstly, there exists a minimum field value $B_{\rm min}$ arising from points in the lattice such as that labelled (a). The overlapping of flux lines means that the flux density does not falls to zero anywhere in the lattice. Secondly, there is a maximum field due to the vortex cores at points such as (b). Below this field there is a long tail, since the high field values only exist in a narrow region of space around the core. There is thirdly a peak in $p(B)$ at a field $B_{\rm pk}$ a little below the mean value $B_{\rm av}$, which arises from points lying close to the minimum on a line connecting two vortex cores, such as (c). Here there exists a large region having a slow spatial variation of $B(r)$, giving rise to the van Hove type singularity. The precise details of $p(B)$ will depend on the symmetry of the lattice (triangular or square) and the values of ξ, λ and a (Sidorenko *et al.* 1990). Probability distributions of this type have been observed in a number of conventional and high-T_c superconductors using μSR, for examples see (Herlach *et al.* 1990, Riseman *et al.* 1995, Lee *et al.* 1993).

The form of $p(B)$ may easily be obtained from a simple numerical simulation, which is often most conveniently performed using reciprocal space. For an ideal vortex line lattice the internal flux density will be periodic and may therefore be expressed as a Fourier series:

$$B(r) = \langle B \rangle \sum_{\mathbf{G}} b_G \exp(i\mathbf{G} \cdot \mathbf{r}) \qquad (2)$$

where **G** is a vector of the reciprocal lattice and the mean flux density is denoted $\langle B \rangle$. In the London limit, where the influence of the cores is neglected, the Fourier components are given by (Tinkham 1975):

$$b_G = \frac{1}{1 + \lambda^2 |\mathbf{G}|^2} \tag{3}$$

from which $p(B)$ may easily be deduced.

In the London limit the penetration depth and lattice spacing may easily be determined from $p(B)$ provided one knows the symmetry of the lattice. This can be determined by the detailed form of $p(B)$ (Sidorenko *et al.* 1990). To distinguish triangular from square morphologies in the Abrikosov limit ($H \sim H_{c_2}$) it is possible, following the analysis of Sidorenko *et al.* (1990). to define a quantity

$$\gamma = \frac{B_{\text{core}} - B_{\text{pk}}}{B_{\text{pk}} - B_{\text{min}}} \tag{4}$$

which for a hexagonal lattice gives $\gamma = 8$ while for a square lattice gives $\gamma = 2.5$ (Aegerter*et al.* 1998). Various features of $p(B)$ scale as λ^{-2}, including the root of the second moment of the distribution

$$\langle \Delta B^2 \rangle^{1/2} = \left[\int_{\substack{\text{unit} \\ \text{cell}}} \left(B^2(r) - \langle B \rangle^2 \right) dr \right]^{1/2}$$

and also $\langle B \rangle - B_{\text{pk}}$. Using Equations 2 and 3 it can be shown that:

$$\langle \Delta B^2 \rangle^{1/2} = \langle B \rangle \left(\sum_{\mathbf{G} \neq 0} b_G^2 \right)^{1/2} \tag{5}$$

$$= \langle B \rangle \left(\sum_{\mathbf{G} \neq 0} \frac{1}{(1 + \lambda^2 |\mathbf{G}|^2)^2} \right)^{1/2}. \tag{6}$$

For fields

$$H \gg H_{c_1} = \frac{\Phi_0}{4\pi\lambda^2} \ln \frac{\lambda}{\xi},$$

Equation 6 becomes

$$\langle \Delta B^2 \rangle^{1/2} = \left(\frac{0.00371 \Phi_0^2}{\lambda^4} \right)^{1/2},$$

so that λ may in principle be easily extracted from the width of $p(B)$, that is $\langle \Delta B^2 \rangle^{1/2}$. It is worth noting that in extreme type II superconductors ($\lambda \gg \xi$) such as the high-T_c materials, at low applied fields (where the cores can be neglected) the high field tail in $p(B)$ extending out to B_{core} is very long and low in value. In real experiments this means that even for very high statistics it is difficult to resolve from the noise the signal arising from the superconductor at fields around the core field, so that the width of the curve is systematically underestimated. This can in turn lead to overestimates of λ. In this instance it is usually better to estimate λ by modelling the entire $p(B)$ at available fields, allowing for this reduced waiting at higher fields, or by using (for a triangular lattice) via (Song *et al.* 1993, Song *et al.* 1995, Lee *et al.* 1993):

$$\langle B \rangle - B_{\text{pk}} = \frac{2}{3} \ln 2 \frac{\Phi_0}{4\pi\lambda^2}$$

where $\langle B \rangle$ is best determined by magnetisation measurements on the same crystals at the same applied field.

At higher applied fields the influence of the cores becomes more significant, as the vortices are pushed closer together. Thus we have to use more sophisticated models in order to obtain correct values for λ and ξ. In the case of $B \lesssim B_{c_2}$ it is possible to analytically calculate the field distribution $p(B)$ from Abrikosov's solution of the Ginzburg-Landau equations (Sidorenko 1990, Brandt 1997). In a different approach, it is possible to use the scaling function recently derived by Yaouanc *et al.* (Yaouanc *et al.* 1997) to extend the London approximation for the full range of applied fields. Examples of successful application of these different approaches to experimental results may be found in references (Sonier *et al.* 1994, Sonier *et al.* 1997a, Sonier *et al.* 1997b, Sonier *et al.* 1997c, Aegerter *et al.* 1998). In the simplest approximation a term is included in the London form factor to account for the presence of the normal state cores so that Equation 3 becomes

$$b_G = \frac{\exp(-\xi^2 G^2/4)}{1 + \lambda^2 |\mathbf{G}|^2}. \tag{7}$$

An application of this approach to a polycrystalline sample of YNi_2B_2C can be found in Cywinski 1995, where the influence of the core size on the field dependence of $\langle \Delta B^2 \rangle^{1/2}$ was used to extract values of λ and ξ, which could be compared to values estimated from magnetisation measurements. A study on single crystals of the anisotropic conventional superconductor $NbSe_2$ has been carried out to investigate the magnetic field dependence of the vortex-core radius and penetration depth (Sonier 1997b). The μSR spectra were fitted in the time domain using a field distribution generated from a Ginzburg-Landau model, which included terms to describe the core cut-off in $p(B)$. In agreement with scanning-tunnelling microscopy (STM) studies, a dependence of the core radius on field was demonstrated in this material.

We conclude this section on ideal vortex lattices with a note concerning measurements on polycrystalline or powder samples. Even for the intrinsically isotropic materials which we have discussed so far, small crystallites can have an associated shape anisotropy. This will cause different average internal flux densities for different orientations of the crystallites relative to the applied field, due to demagnetisation effects Taken over a powder average of random orientations, the superposition of many signals with different internal field values will lead to μSR signals quite different from that expected for an ideal single crystal. Caution must therefore be exercised when extracting values of λ and ξ. A detailed treatment of this type of analysis for an intrinsically anisotropic material is given in reference (Weber *et al.* 1993).

4 The influence of pinning of rigid vortex lines

In this section we will look briefly at the influence on the μSR signal of distortions of the vortex lattice due to pinning. It is worth noting at this point that the influence of pinning can be quite different in highly anisotropic systems in which the vortex lines are 'soft', which we will discuss later. Here we assume that the vortex lattice in the absence of pinning is a conventional lattice of rigid vortex lines.

The influence of material defects as pinning sites, which trap the vortex lines, is particularly effective when the extent of the pinning site is of the order of the vortex core.

In the mixed state it is energetically favorable for vortex lines to have cores which coincide with areas of the samples where the order parameter is suppressed, since condensate energy is not lost from these volumes. There is thus an effective force of attraction between a pinning site and a vortex line. The effectiveness of this pinning site depends upon the relative strength of the interaction U_p compared to the energetic cost of a local elastic deformation of the lattice, $U_e \sim 1/2C\alpha^2$ per unit volume, where C is an elastic constant of the lattice and α is the local strain. The value of the effective elastic constants of the lattice depends on material parameters and the conditions of the experiment (e.g. λ, T, B) (Blatter *et al.* 1995).

The effect of pinning induced deformations of an ideal vortex lattice on the μSR signal have been studied in detail by Brandt 1988. A general feature is a smearing of the sharp features in $p(B)$ at $B_{\rm min}$, $B_{\rm core}$ and $B_{\rm pk}$. Disorder of this sort always acts to *increase* the width of $p(B)$, so can lead to an *underestimate* of the value of λ if formulae such as Equation 6 are used without proper consideration of the rôle of disorder. It was shown by Brandt that the effects are in general equivalent to a convolution of $p(B)$ with a Gaussian function representing the effects of disorder in the lattice:

$$P_d(B) = \int \frac{1}{2\pi\sigma_d} \exp\left[-\frac{1}{2}\left(\frac{B-B'}{\sigma_d}\right)^2\right] p(B)dB' \tag{8}$$

where σ_d may be related to the root mean square displacement $\langle u^2\rangle^{1/2}$ of a vortex line about its mean position. Such analysis has been successfully applied to studies of disorder in the moderately anisotropic high-T_c superconductor $YBa_2Cu_3O_{7-\delta}$ by Riseman *et al.* (1995).

5 Anisotropic superconductors

The vortex state in anisotropic superconductors becomes more complex than in isotropic systems. The flow of anisotropic supercurrents leads to vortex structures which are a function of the angles between the applied field and the crystallographic axes, requiring different interpretation if characteristic length scales are to be determined. Highly anisotropic systems may also give rise to highly exotic vortex structures and behaviour, which μSR is a powerful tool to study.

To illustrate some of the general properties of anisotropic superconductors, we begin with the high-T_c superconductors, such as $YBa_2Cu_3O_{7-\delta}$ (YBCO). The high-T_c cuprate superconductors are highly layered materials in which the conduction electrons are confined to the copper-oxide planes, so that one could schematically represent them as a stack of two-dimensional conducting planes, as in Figure 5. With a Cartesian frame aligned with the crystallographic axes three independent current densities may be defined, J_1,J_2 and J_3. High-T_c materials can to a good approximation be considered to be uniaxial, that is,$J_1 \sim J_2$, $J_1, J_2 \gg J_3$, although we shown below that this is not strictly correct. The effective screening of each current density is different, so we may associate with each J_i a penetration depth λ_i. The anisotropy parameter of a material is then defined as $\gamma = \lambda_3/\lambda_1$ in a uniaxial system. It can be seen from Figure 5 that different orientations of the field, perpendicular and parallel to the planes, involve different components of the

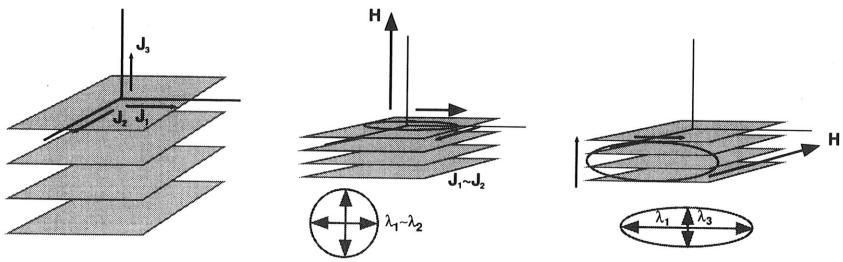

Figure 5. *A schematic representation of the superconducting anisotropy in a layered material such as the high-T_c materials; (a) defines the geometry of the currents and (b), (c) show the cases of the field directed perpendicular to the planes and directed within the planes respectively*

current density, so that the resulting cross-section of a flux line will depend on the orientation of the field. The resulting electromagnetic interactions between flux lines will also be anisotropic, so in general the flux line lattice will be a distorted hexagonal or distorted square arrangement (Figure 6a and 6b).

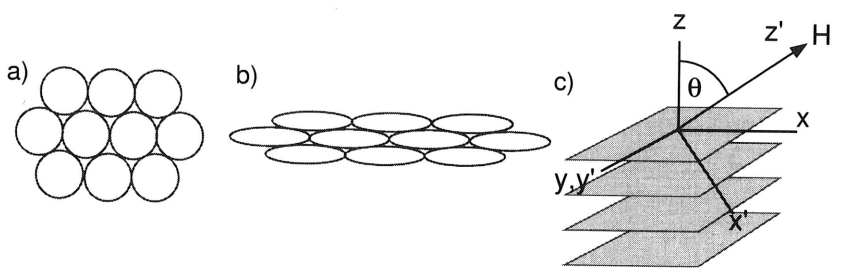

Figure 6. *The cross-section of a flux lattice in a uniaxial anisotropic superconductor, with the field applied (a) perpendicular and (b) parallel to the planes. In (c) we show the geometry for solving the London equation (see text).*

In trying to find solutions to an anisotropic vortex system, it is useful to define an effective mass tensor

$$\underline{\Lambda} = \begin{pmatrix} m_1 & 0 & 0 \\ 0 & m_2 & 0 \\ 0 & 0 & m_3 \end{pmatrix} \tag{9}$$

where $m_i = M_i/M_{\rm av}$ and $M_{\rm av} = (M_1 M_2 M_3)^{1/3}$. For the field directed along one of the principal axes x_i the effective penetration depth is then given by $\lambda_{\rm eff}^{-1}(B \parallel x_i) = (M_j M_k)^{1/2}$. The London equations have been solved by Thiemann *et al.* (1989) for the case of a uniaxial system. For simplicity the case is considered where the field is rotated away from the axis perpendicular to the planes, about one of the other principal axes: in Figure 6c) we show a frame x', y', z' rotated about one of the principal axes (y-axis), where H is applied along the z' axis. The Fourier components of the internal flux density were determined for arbitrary rotation θ, and these can be used to simulate the probability distribution $p(B, \theta)$. It is interesting to note that for the general case of the field directed

away from a principal axis, there are components of the field which are perpendicular to the applied field direction. The results of Thiemann *et al.* lead to the following angular dependence of the linewidth (Forgan *et al.* 1990, Cubitt *et al.* 1993):

$$\langle \Delta B^2 \rangle^{1/2}(\theta) = \langle \Delta B^2 \rangle^{1/2}(0)(\cos^2\theta + \frac{1}{\gamma^2}\sin^2\theta)^{1/2} \tag{10}$$

where $\gamma = \lambda_3/\lambda_1$. (We bring to the attention of the reader a minor error in Thiemann *et al.* (1989), corrected in the Appendix of Cubitt *et al.* (1993). This was shown to be a good description of the angular dependence of the second moment of $YBa_2Cu_3O_{7-\delta}$ (Forgan 1990).

To a first approximation $YBa_2Cu_3O_{7-\delta}$ appears to be uniaxial, since the orthorhombic symmetry leads to twinned single crystals in which twin boundaries are formed where the a and b axes meet along the same direction in the sample. Any differences due to in-plane a-b anisotropy are thus impossible to detect in twinned crystals. Recently large untwinned single crystals of $YBa_2Cu_3O_{7-\delta}$ suitable for μSR have become available, and in these it is possible to measure the angular variation of $\langle \Delta B^2 \rangle^{1/2}(\theta)$ as the field rotates between the a- and b-directions (Ager *et al.* 1999). An example is given in Figure 7, where the measured angular variation of $\langle \Delta B^2 \rangle^{1/2}(\theta)$ is shown for rotation of the field both between the $c-$ and a-axis and also between the a- and the b-axis. The variation of the latter is small since anisotropy ratio $\gamma_{ab} = \lambda_a/\lambda_b$ is much lower than $\gamma_{ac} = \lambda_c/\lambda_a$. b

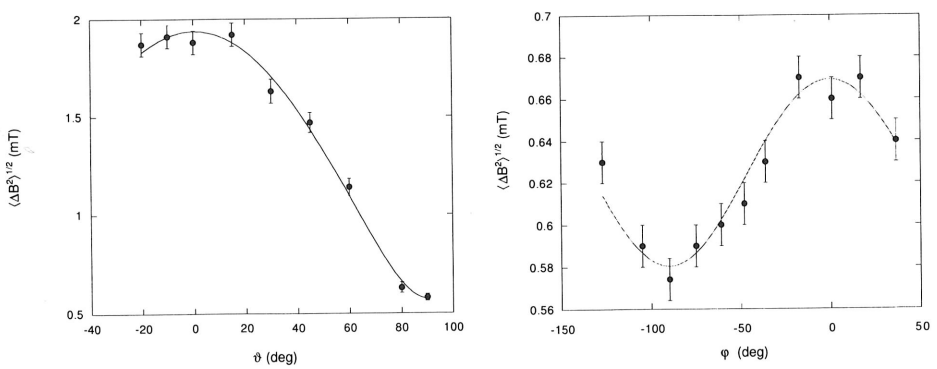

Figure 7. *Angular dependence of the second moment* $\langle \Delta B^2 \rangle^{1/2}(\theta)$ *in untwinned single crystals of* $YBa_2Cu_3O_{7-\delta}$. *The fits are to Equation 10 (Ager et al. 1999).*

The case of measurements on powder samples of anisotropic uniaxial superconductors was treated by Barford and Gunn (1988). It was shown that in the London limit for an hexagonal lattice at $H_{c_1} \lesssim H << H_{c_2}$, the second moment of $p(B)$ is given by

$$\langle \Delta B^2 \rangle^{1/2} = \left(\frac{0.00371 F \Phi_0^2}{\lambda_1^4} \right)^{1/2},$$

where F is a function of the anisotropy γ, with $F \approx 0.44$ for $\gamma \gtrsim 5$. This means that measurements on powders of highly anisotropic systems can be used to determine the in-plane penetration depth λ_1 without the need for any detailed measurements of the anisotropy, other than ensuring that it is moderately large. Measurements on high quality powder

samples are thus extremely useful for studies of the systematic variation of penetration depth within and between families of exotic supeconductors (Uemura *et al.* 1988, Uemura *et al.* 1989, Uemura *et al.* 1991, Keller *et al.* 1992, Zimmerman *et al.* 1993). It should be noted that extracting precise measurements of penetration depth using powders is rather difficult, due to the possible complications from demagnetisation factors, pinning induced broadening (or even narrowing, as discussed in the following section), and the fact that only the second moment is readily accessible to analysis, which may also be affected by finite statistical effects. It is the author's opinion that the strength of this method is to make comparisons of the relative trends of penetration depths between systems, rather than yielding highly exact and precise values. This is true to some extent even for single crystal measurements, where precise values of λ depend on the validity of the model used to model the data, and a correct assessment of the effect of various influences on the vortex lattice.

6 Exotic vortices in highly anisotropic systems

Systems of high anisotropy, such as the high-T_c superconductors, may exhibit a greater variety of vortex structures than conventional systems. In the high-T_c's for example, a combination of high anisotropy γ and high Ginzburg-Landau parameter $\kappa = \lambda/\xi$ leaves the vortex lattice highly susceptible to disruption by pinning or thermal fluctuations (Blatter *et al.* 1995). The latter is particularly effective due to the high transitions temperatures, although thermal influence is thought be to important in even more extreme low-T_c systems such as some of the organic superconductors (Lee *et al.* 1997a, Taniguchi *et al.* 1998). A good model of a vortex line in a layered anisotropic system is one consisting of a string of two-dimensional pancake vortices, as illustrated in Figure 8 (Kossler *et al.* 1998). The vortices in different layers are coupled by electromagnetic forces and are often additionally coupled by Josephson tunnelling currents flowing between the layers (Blatter *et al.* 1995, Lawrence and Doniach 1971). The case of strong coupling produces rigid line-like structures which are for many purposes indistinguishable from conventional vortex lines. As the inter-layer coupling exceeds the intra-layer coupling, however, the vortex lines become increasingly flexible, developing a more quasi-2d character.

It is instructive to consider the effect of static deformations of flexible vortex lines on the probability distribution $p(B)$. Brandt has shown that disorder of this type will always

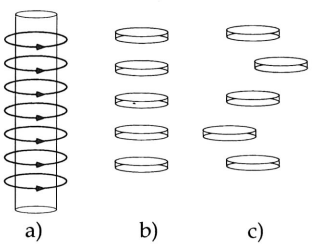

Figure 8. *Schematic representations of flux vortices in (a) systems approaching the isotropic limit where a conventional view of a vortex line is valid, (b) highly layered anisotropic systems with strong inter-layer coupling and (c) highly layered anisotropic systems with weak inter-layer coupling.*

narrow $p(B)$ (Brandt *et al.* 1991). This occurs principally due to a truncation of the high field tail in $p(B)$, which may understood as follows. The high fields arise from regions close to the centre of a vortex, but the onset of disorder along the vortex line (Figure 8c) causes a washing out of these high fields since the pancake cores in neighbouring layers no longer coincide. The width of the distribution of fields about the average is thus reduced. This is in contrast to the case of disorder in a lattice of rigid vortex lines, where the width of $p(B)$ is always increased. For the case of flexible vortex lines, failure to take correct account of the influence of disorder on the vortex lattice may lead to an underestimate of $\langle \Delta B^2 \rangle^{1/2}$ and thus to an *overestimate* of λ. An example of narrowing of $p(B)$ due to disorder is provided by the high-T_c material $Bi_2Sr_2CaCu_2O_{8+\delta}$ (BSCCO) (Harshman *et al.* 1991, Harshman *et al.* 1993, Lee *et al.* 1993, Aegerter *et al.* 1996). At low fields a signal typical of a vortex line lattice is measured, but at fields above approximately 65mT the linewidth rapidly narrows, reflecting the onset of disorder along the vortex lines. This is clearly illustrated in Figure 9a which shows the field dependence of the skewness parameter, $\alpha = \langle \Delta B^3 \rangle^{1/3} / \langle \Delta B^2 \rangle^{1/2}$ derived from the second and third moments of $p(B)$. In this example a value of $\alpha \sim 1.25$ represents the skewness of a $p(B)$ arising from something close to an ideal vortex line lattice. At higher fields the lower values of α reflect a much more symmetric lineshape arising from truncation of the high-field tail of $p(B)$. This is due to a meandering of the vortex lines along their length, stabilised by random point pinning centres in the material which trap short segments of the vortex lines. All measurements were taken after cooling in a field from above T_c to 5K, (Lee *et al.* 1993, Cubitt *et al.* 93a, Aegerter *et al.* 1996).

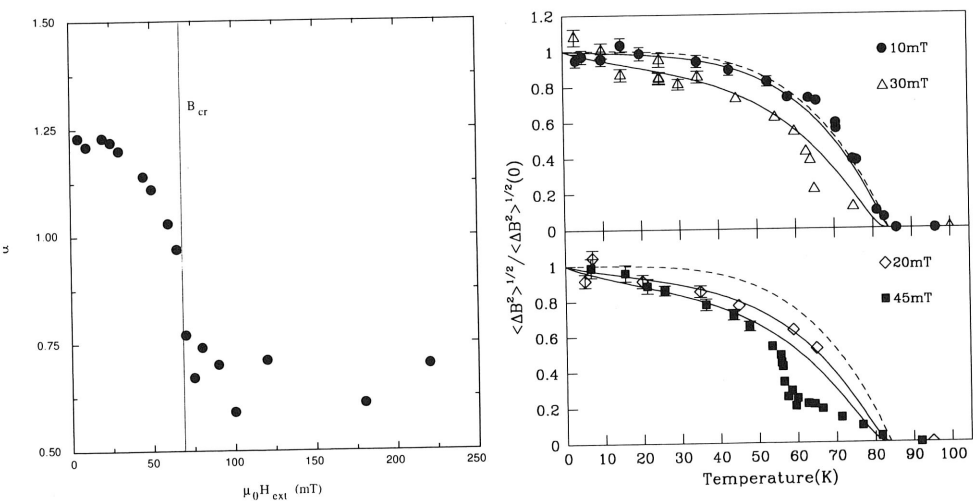

Figure 9. *Examples of the influence of static and dynamic fluctuations on the field probability distribution* $p(B)$ *in the high-*T_c *superconductor* $Bi_2Sr_2CaCu_2O_{8+\delta}$ *(BSCCO). (a) shows the field dependence of the skewness parameter and (b) shows the variation with field of the temperature dependence of the line width. From Aegerter et al. (1996).*

For flexible vortex lines, a dynamic effect similar to the static disordering can arise through thermally induced fluctuations of the vortex positions (Song *et al.* 93, Song *et al.* 95, Lee *et al.* 1993, Lee *et al.* 1995, Lee *et al.* 97a). In BSCCO this may be clearly

observed by an additional narrowing of the lineshape with temperature (Figure 9b). This figure shows the variation with field of the temperature dependence of the line width $\langle \Delta B^2 \rangle^{1/2}(T, B)$ (Lee *et al.* 1995, Lee *et al.* 97a). For an ideal superconductor the temperature variation should simply reflect that of the penetration depth $\lambda(T)$, but here there is additional narrowing of $p(B)$ with increasing temperature due to thermal fluctuations of the vortex positions (see text). The solid lines are fits to the data using a simple model to account for the influence of the thermal fluctuations (Lee *et al.* 1995, Lee *et al.* 1997a). The typical timescale of vortex motion is much shorter than the muon precession period (Song *et al.* 1993, Song *et al.* 95), so the muon experiences an increasingly motionally narrowed field distribution with increasing temperature (Lee *et al.* 1995). The influence of the thermal fluctuations on the field distribution also becomes greater with increasing field, the details of which allow information concerning the form of the vortex fluctuations to be deduced (Lee *et al.* 1995, Lee *et al.* 1997a).

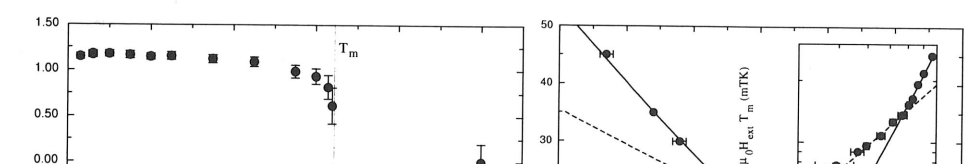

Figure 10. *The effects of vortex lattice melting on the field probability distribution $p(B)$ in (BSCCO). (a) shows the temperature dependence of the skewness parameter of the field distribution, α, measured at 30mT. (b) shows the field dependence of the melting transition $T_m(B)$, showing the good agreement with predictions of theory.*

When the thermal vibrations of the vortices becomes sufficiently large, a transition to a melted vortex liquid state can occur (Brandt *et al.* 1989, Houghton *et al.* 1989, Fisher *et al.* 1991,Glazman *et al.* 1991, Blatter*et al.* 1995, Blatter*et al.* 1996). This can be seen from the very rapid narrowing of the field distribution above a certain temperature $T_m(B)$ in the plots of $\langle \Delta B^2 \rangle^{1/2}(T, B)$ in Figure 9b. This transition from a solid to a vortex liquid state is even more dramatically represented in Figure 10, where the overall shape of $p(B)$ is represented by the skewness parameter $\alpha = \langle \Delta B^3 \rangle^{1/3} / \langle \Delta B^2 \rangle^{1/2}$, (Lee *et al.* 1993, Lee *et al.* 1997a). At fields up to the melting temperature $T_m(B)$ the shape of the distribution is almost unchanged, but at the $T_m(B)$ there is a dramatic truncation of the high-field tail of $p(B)$, reflected in the figure by a change in α. This is most likely due to a combination of increased dynamics and increased vortex line flexibility at $T_m(B)$ (Lee *et al.* 1993, Lee *et al.* 1997a). The dependence of the melting line on field $T_m(B)$ may be determined, and is found to be in good agreement with more sophisticated models of vortex melting, which properly account for the relative importance of Josephson and electromagnetic coupling in this extremely anisotropic system (Lee *et al.* 1997, Blatter *et al.* 1996). A more detailed review of μSRmeasurements on exotic superconductors can be found in Aegerter *et al.* (1997).

7 Studies of the penetration depth

The evaluation of Equation 6 for $H_{c_2} \gg H \gg H_{c_1}$ indicates that the width of the field distribution $p(B)$, $\langle \Delta B^2 \rangle^{1/2}(T) = c/\lambda^2(T)$, where c is a numerical constant which depends on the symmetry of the vortex lattice. In the London limit the penetration depth can be related to the density and effective mass of the superconducting charge carriers by $n_s/m^* \propto \lambda^{-2} \propto \langle \Delta B^2 \rangle^{1/2}$ (Tinkham 1975), so the μSR linewidth is a direct measure of the ratio n_s/m^*. This has lead to a large number of studies on systematic trends of $n_s/m^*(0)$ in and between families of superconductors (e.g. Uemura *et al.* 1988, Uemura *et al.* 1989, Uemura *et al.* 1991, Keller *et al.* 1992, Zimmerman *et al.* 1993) and also of the temperature variation of $\lambda(T)$ (e.g. (Keller *et al.* 1992, Zimmerman *et al.* 1993, Sonier *et al.* 1994, Sonier *et al.* 1997a, Sonier *et al.* 97b, Sonier *et al.* 1997c). For many purposes a detailed study of the lineshapes of single crystals is not necessary, and powder samples are used. A common approach is to approximate the μSR lineshape from powder samples as a Gaussian distribution, which may be simply analysed in the time domain using a Gaussian relaxation, which is often found to provide a very good description of the data. This approach yields a Gaussian linewidth which is proportional to n_s/m^*. More detailed approaches to study the temperature-dependence and field-dependence of λ in single crystals have been performed, using fits in the time domain to theoretical models of $p(B)$ (Sonier *et al.* 1994, Riseman *et al.* 1995, Sonier *et al.* 1997a, Sonier *et al.* 1997b, Sonier *et al.* 97c). A study of the high-T_c material YBCO demonstrate a linear dependence of $\lambda(T)$ on temperature, consistent with zero field microwave cavity measurements and the prediction of d-wave models of superconductivity (Sonier *et al.* 1994). More recent measurements on YBCO have found a linear dependence of $\lambda(0)$ on applied field H (Sonier *et al.* 97a), which has been attributed to a strong non-linear response related to unconventional pairing in the superconducting state.

8 Summary

It is worth noting that while μSR is an invaluable and unique method more making comparative measurements of the parameters of the superconducting state, the absolute determination of the penetration depth is fraught with possible sources of error, since these are always extracted by making assumptions about the vortex-lattice structure. We therefore briefly re-iterate some of the points that must be considered in making such measurements. For the case of a conventional vortex lattice one must perform single crystal experiments to determine the symmetry of the lattice. The influence of the finite core size should also be determined. It should furthermore be borne in mind that finite statistics could lead to an underestimate of the width of the distribution, and if the whole lineshape is not modelled, then λ should at least be self-consistently checked from various features of the measured lineshape. The lineshapes should also be studied for the influence of pinning-induced disorder, which for a lattice of rigid vortex lines will broaden the lineshape. For powder samples care must be taken to treat the effects of shape anisotropy or intrinsic anisotropy in the powder averages. In studies of more exotic highly anisotropic materials, the flexible flux lines are highly susceptible to thermally-induced (dynamic) or pinning-induced (static) deformations, which in this case tend to narrow the lineshapes, which may give very misleading values of the penetration depth if not properly

accounted for. This can also lead to variations of lineshape with temperature and field which are heavily influenced by the changes and evolution of the vortex lattice, and which do not simply reflect the penetration depth. Given these reservations, values of parameters extracted from other techniques such as STM, magnetisation studies, neutron scattering and microwave absorption measurements are often found to be in very good agreement with those determined using μSR. The extreme sensitivity of the μSR lineshapes to subtle changes in the vortex structure such as the symmetry and degree and type of disorder, make the technique extremely powerful for the study of the vortex state, and one which is highly complementary to other methods such as neutron scattering, STM and Bitter decoration techniques.

Acknowlegements

The many people who have contributed to my understanding of this subject are far too numerous to mention. I would however like to give particular thanks to Ted Forgan, Bob Cubitt, Christof Aegerter and Hugo Keller, for their encouragement, support, insight, and inovative approach to the application of μSR to studies of the vortex state.

References

Ager C, 1998, University of St. Andrews, unpublished.
Aegerter C M *et al.* , 1996, *Phys Rev* **B 54** *15661.*
Aegerter C M and Lee S L , 1997, *Appl Mag Reson* **B 13** 75.
Aegerter C M*et al.* , 1998, *J Phys Cond Mat* **10** 7445.
Barford W and Gunn J M F, 1988, *Physica C***156** 515.
Blatter G *et al.* , 1991, *Rev Mod Phys* **66** 3213.
Blatter G, Geshkenbein V, Larkin A and Nordborg H, 1996, *Phys Rev.***B 54** 15661.
Brandt E H, 1988, *J Low Temperature Physics***73** 355.
Brandt E H, 1989, *Phys Rev Lett* **63** 1106.
Brandt E H, 1995, *Phys Rev Lett* **66** 1125.
Brandt E H *et al.* , 1997, *Phys Rev Lett* **78** 2208.
Cubitt R *et al.* , 1993, *Physica C,* **213** 126.
Cubitt R *et al.* , 1993, *Nature* **365** 407.
Cywinksi R *et al.* , 1995, *Physica C* **233** 273.
Fisher D S, Fisher M P A and Huse D A, 1991, *Phys Rev* **B 43** 130.
Forgan E M *et al.* , 1990, *Hyperfine Interactions* **63** 71.
Glazman L I and Koshelev A E, 1991, *Phys Rev* **B 43** 2835.
Harshman D R *et al.* , 1991, *Phys Rev Lett* **67** 3152.
Harshman D R *et al.* , 1993, *Phys Rev B* **47** 2905.
Herlach D *et al.* , 1990, *Hyp Int* **63** 41.
Houghton A, Pelcovits R A, and Sudbø, 1990, *Phys Rev* **B 40** 6763.
Kossler W J *et al.* , 1998, *Phys Rev Lett* **80** 592.
Lawrence W E and Doniach S, 1971, *Proceed of Twelth Int Conf on Low Temperature Physics*, Kyoto 1970 361 editor Kanda E (Keigaku, Tokyo).
Lee S L*et al.* , 1993, Phys Rev Lett **71** 3862.
Lee S L *et al.* , 1995, *Phys Rev Lett* **75** 922.
Lee S L *et al.* , 1997, *Phys Rev Lett* **79** 1563.

Lee S L *et al.* , 1997, *Phys Rev B* **55** 5666.
Riseman T *et al.* , 1995, *Phys Rev.***B 52** 10569.
Schneider T and Keller H, 1992, *Phys Rev Lett* **69** 3374.
Sidorenko A D *et al.* , 1990, *Hyp Int* **63** 49.
Song Y -Q, *et al.* , 1993, *Phys Rev Lett* **70** 3127.
Song Y -Q, *et al.* , 1995, *Physica* **C 241** 187.
Sonier J *et al.* , 1994, *Phys Rev Lett* **72** 744.
Sonier J *et al.* , 1997, *Phys Rev B* **55** 11789.
Sonier J *et al.* , 1997, *Phys Rev Lett* **79** 1742.
Sonier J *et al.* , 1997, *Phys Rev Lett* **79** 2875.
Taniguchi H *et al.* , 1988, *Phys Rev* **B 57** 3623.
Thiemann S L *et al.* , 1989, *Phys Rev B* **39** 11406.
Tinkham M, 1975, *Introduction to Superconductivity*, Malabar, Florida, USA:McGraw-Hill.
Uemura Y J *et al.* , 1998, *Phys Rev* **B 38** 909.
Uemura Y J*et al.* , 1989, *Phys Rev Lett* **62** 2317.
Uemura Y J *et al.* , 1991, *Phys Rev Lett* **66** 2665.
Weber M *et al.* , 1993, *Phys Rev B* **48** 13022.
Yaouanc A *et al.* , 1997, *Phys Rev B* **55** 11107.
Zimmerman P *et al.* , 1993, *Phys Rev B* **52** 541.